J. Membrane Biol. 151, 225–235 (1996)

The Journal of
Membrane
Biology

N-type Inactivation in the Mammalian *Shaker* K^+ Channel Kv1.4

T.E. Lee[1], **L.H. Philipson**[2], **D.J. Nelson**[1,2,3]
[1]Departments of Neurology, [2]Medicine, [3]Pharmacological and Physiological Sciences, The University of Chicago, Chicago, IL 60637

Received: 24 August 1995/Revised: 7 February 1996

Abstract. Mammalian voltage-gated K^+ channels are oligomeric proteins, some of which may be composed in vivo of subunits derived from several similar genes. We have studied N-type inactivation in the rapidly inactivating Kv1.4 channel and, in specific, heteromultimers of this gene product with Kv1.5 noninactivating subunits. Heteromultimeric channels were analyzed for the stoichiometry of Kv1.4:Kv1.5 subunits by observing shifts in the midpoints of steady-state availability from that of homomultimeric channels. This analysis was employed to examine inactivation of heteromultimeric channels expressed in *Xenopus* oocytes using two model systems: by expression of a Kv1.4–Kv1.5 tandem fusion construct and by coexpression of native Kv1.4 and Kv1.5 channels across a wide relative concentration range of microinjected mRNA. Additionally, inactivation was examined in coexpression experiments of N-terminal deletion mutants of Kv1.4. We found that (i) a single inactivating subunit conferred inactivation in all hetero-multimers studied; (ii) the rate of inactivation could not be distinguished in channels containing two inactivating subunits from those containing one inactivating subunit; and (iii) large deletions in the linker region between the N-terminal inactivation region and the first membrane-spanning domain had no effect on the rate of inactivation. These data confirm the importance of the proximal N-terminal region in the inactivation of mammalian Kv1.4 channels, and suggest that the inactivation particle remains in close proximity to the permeation pathway even when the channel is in the open state.

Key words: *Xenopus* oocyte — Voltage clamp — Mutagenesis — Heteromultimers — Ion channels

Correspondence to: D.J. Nelson

Introduction

Potassium (K^+) channels are ubiquitous ion channel proteins that regulate diverse cellular functions including excitability, secretion, motility and transport. The mammalian voltage-gated K^+ channels are structurally related to the *Drosophila Shaker* gene, part of a large gene superfamily (Jan & Jan, 1994). Isoforms of *Shaker*-type K^+ channels, when expressed as homomultimers, can be grouped as having ''fast'' or ''slow'' rates of current inactivation in response to maintained depolarization (Isacoff, Jan & Jan, 1993). A molecular model for fast inactivation in the *Drosophila* K^+ channel ShB was first proposed by Hoshi and colleagues (Hoshi, Zagotta & Aldrich, 1990). In this model, the N-terminus of a subunit forms a structure that functions as a cytoplasmic gate capable of blocking the flow of K^+ ions, similar to the ''ball and chain'' model first proposed to explain inactivation in voltage-dependent Na^+ channels (Armstrong & Bezanilla, 1977). Support for the ball and chain model in ShB came from analysis of N-terminal deletion mutations and, additionally, from the observation that peptides derived from the N-terminal sequence of *Shaker* K^+ channels can act as effective channel blockers (Murrell-Lagnado & Aldrich, 1993*a*,*b*; Zagotta, Hoshi & Aldrich, 1990). In the ball-and-chain model, the inactivation particle effects inactivation by diffusing into the mouth of the channel, where diffusion is limited by a peptide tether of approximately 60 residues that connects the inactivation particle to the mouth of the channel. This model is supported by a change in inactivation rate when the concentration of inactivation particles is modified either by: (i) changing the length of the peptide tether using mutagenesis (Hoshi et al., 1990); (ii) changing the concentration of exogenous inactivation peptide applied to the cytoplasmic side of inactivation deficient mutant channels (Zagotta et al., 1990), or (iii) varying the

number of inactivating subunits within a tetrameric channel (MacKinnon, Aldrich & Lee, 1993).

An N-terminal mechanism has been proposed for the inactivation observed in the mammalian *Shaker* homologue, Kv1.4 (Ruppersberg et al., 1991; Tseng & Tseng-Crank, 1992; Tseng-Crank et al., 1993). We investigated the inactivation mechanism of Kv1.4 and found that it appears to be due to a tethered particle which remains in close proximity to the channel pore. Unlike the inactivation properties observed in the *Drosophila* channel, inactivation is present in the mammalian channel even when the entire peptide tether is deleted. Secondly, the rate of inactivation in three types of heteromultimeric Kv1.5:Kv1.4 channels was analyzed by taking advantage of the large difference in steady-state availability between Kv1.4 and Kv1.5. The results suggest that the rate of inactivation was nearly constant for one to two inactivation gates per channel. Therefore, although inactivation in Kv1.4 is structurally dependent upon the presence of a cytoplasmic N-terminal domain, as observed in ShB *shaker* channel, the precise molecular interactions producing inactivation appear to be somewhat different between the two gene families.

Materials and Methods

In vitro Mutagenesis

The wild-type channels Kv1.4 - pSP64T, the hKv1.5 - pSP64T, deletion mutants $hKv1.4_{\Delta 28\text{-}231}$, and hKv1.4 - Kv1.5 - pSP64T constructions have been described previously (Lee et al., 1994; Philipson et al., 1991; Philipson et al., 1990). The deletion mutant $Kv1.4_{\Delta 2\text{-}283}$ was formed by polymerase chain reaction (PCR) amplification of the mutant gene from the $Kv1.4_{\Delta 28\text{-}283}$-pSP64t construct, using two synthetic primers and *Vent* DNA polymerase (New England Biolabs, Beverly, MA). The sequence of the forward primer oligo was GTAGGCGGATCCCCCGGCCATGGAAGCCCTCCCCGAGAATGAATT which matched $Kv1.4_{\Delta 28\text{-}283}$ beginning at residue A27, and added a *Bam*HI restriction site, the Kozak initiation sequence (Kozak, 1989), and an ATG start codon. The sequence of the reverse primer was ATGACCATGATTACGAATTC which overlapped the *Eco*I restriction site within the vector. The PCR product was digested with *Bam*HI and *Eco*RI and ligated into a *Bgl*II/*Eco*RI prepared pSP64t vector (Krieg & Melton, 1987). The pSP64t vector (Krieg & Melton, 1987) was prepared by digestion with *Bgl*II and *Eco*RI restriction enzymes and separated from the smaller digestion fragments by agarose gel electrophoresis. Mutations were confirmed by sequencing, restriction digests, or both.

Harvesting Oocytes

Adult female *Xenopus laevis* (Xenopus I, Ann Arbor, MI) were maintained in deionized water at room temperature (18 to 24°C) and oocytes harvested according to published methods (Marcus-Sekura & Hitchcock, 1987).

Defolliculated oocytes were injected with cRNA and incubated at 18°C in petri dishes on a film of agar in OR-2 solution which contained (in mM): 83 NaCl, 2.5 KCl, 1 $CaCl_2$, 1 $MgCl_2$, 1 Na_2HPO_4, 1 Na-pyruvate, and 5 HEPES (4-(2-hydroxyethyl)-1-piperazineethanesulfonic acid), pH 7.6, supplemented with 100 mg/ml gentamicin.

Preparation and Expression of cRNA

cRNA for injection into *Xenopus* oocytes was prepared using the ''mCAP mRNA Capping Kit'' (Stratagene Cloning, LaJolla, CA). Plasmid DNA was linearized with *Eco*RI (except where otherwise indicated) followed by incubation with proteinase K (Promega, Madison, WI) and phenol-chloroform extraction. Coinjected Kv1.4 and Kv1.5 cRNA was prepared by mixing all required cRNA ratios at one time from the same solution of cRNA; aliquots were then stored at −70°C for future use. Oocytes were microinjected with 50 nL of a solution containing cRNA at a concentration of 0.01 μg/μl for Kv1.4, Kv1.5, and coinjections of Kv1.4 and Kv1.5$Kv1.4_{\Delta 2\text{-}283}$ cRNA was injected at a concentration of 0.01 μg/μl, $Kv1.4_{\Delta 28\text{-}283}$ cRNA was injected at a concentration of 0.1 μg/μl, and the 30:1 ($Kv1.4_{\Delta 2\text{-}283}$:$Kv1.4_{\Delta 28\text{-}283}$) coinjections of cRNA were carried out using a concentration of 2.1 μg/μl. The Kv1.4 and Kv1.5 wild-type and mutant constructs expressed with similar efficiency in *Xenopus* oocytes. An injection of 0.5 ng of cRNA produced 5.4 ± 2.1 μA ($n = 4$) for Kv1.5 and 9.5 ± 3.1 μA ($n = 4$) Kv1.4 two to three days post injection into *Xenopus* oocytes (10 ng of $Kv1.4_{\Delta 2\text{-}283}$ cRNA produced 1.2 μA ($n = 2$), 10 ng of $Kv1.4_{\Delta 28\text{-}283}$ cRNA produced 1.2 μA ($n = 2$)).

Data Acquisition and Analysis

Current recordings were made using the two-microelectrode voltage-clamp technique. Data were acquired using the Warner OC-725 amplifier (Warner Instruments, Hamden, CT). The output of the amplifier was low-pass filtered through an eight-pole Bessel filter (Frequency Devices, Haverhill, MA) at 500 Hz and digitized at 1,000 Hz. Data were stored and analyzed with an IBM PC compatible computer. Currents were recorded two-to-four days following cRNA injection. Microelectrodes filled with 3M KCl had resistances of 0.3–0.7 MΩ. Currents were recorded in standard OR-2 solution without pyruvate or gentamycin.

In those experiments examining the rates of current inactivation, all inactivating currents were isolated using a combination of prepulse and nonprepulse protocols recording from a holding potential of −100 mV. Inactivating currents were initially removed using a double pulse protocol consisting of a prepulse to +40 mV for 1,000 msec followed 500 msec later by a test pulse to +40 mV for 2,000 msec. Recovery from inactivation for the transient component of the current during the 500 msec interval was negligible. A second current recording was made in the absence of a prepulse during a single-voltage step to +40 mV for 2,000 msec. The transient component of the current removed during the prepulse protocol was obtained by subtracting prepulsed current from nonprepulsed current. Current decays were analyzed as a sum of exponentials by a Fourier method (Provencher, 1976) that determined the number, amplitudes, and time constants of the components. Summary data are expressed as means ± SEM with the number of experiments in parentheses.

Results

N-type Inactivation in Kv1.4

A series of deletion mutants was constructed to further characterize the mechanism of fast current inactivation

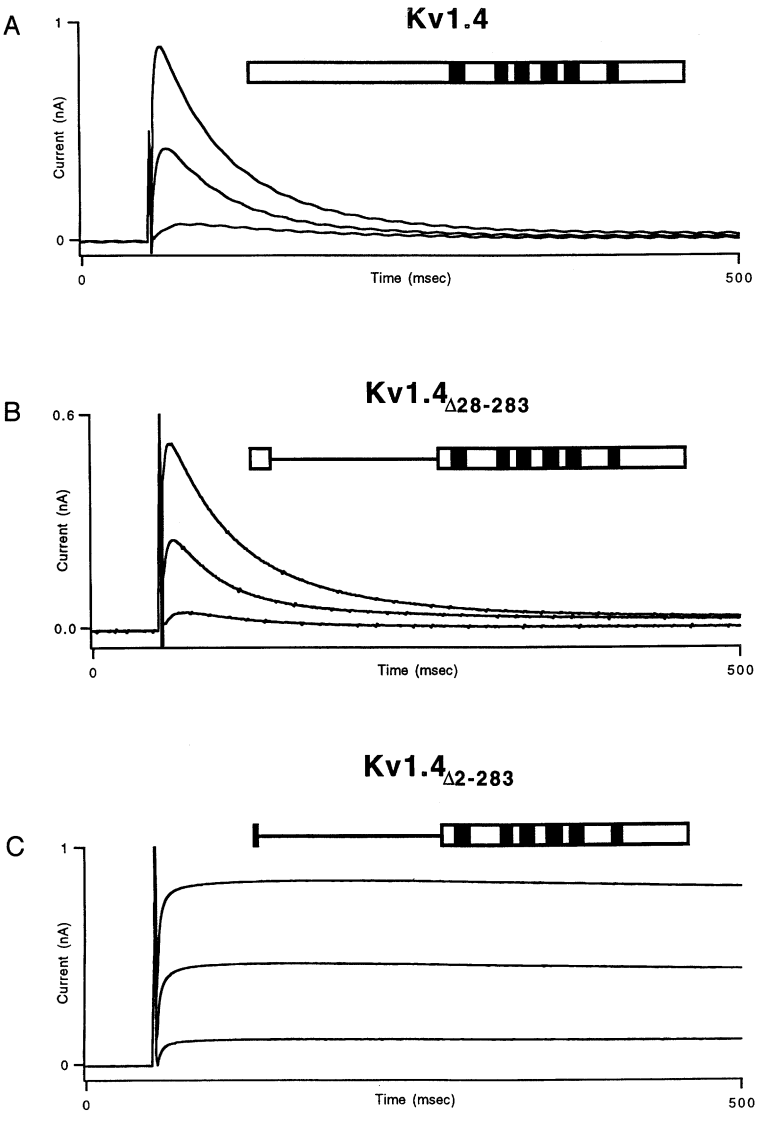

Fig. 1. Kv1.4 inactivates by an N-terminal mechanism. Representative currents for Kv1.4 wild-type channels (*A*), $Kv1.4_{\Delta 28\text{-}283}$ deletion mutant channels in which 255 residues have been deleted from the N-terminus (*B*), and $Kv1.4_{\Delta 2\text{-}283}$ deletion mutant channels in which the 26 additional amino-terminal residues were deleted (*C*). Currents were recorded during voltage steps from −60 to +40 mV in increments of 20 mV from a holding potential of −80 mV, with an interpulse interval of 10 sec. The subunit primary structure is schematically represented above each current record with the filled regions designating the six putative transmembrane helices. Regions which have been deleted are represented by a horizontal line.

observed for Kv1.4 channels. Deletion of more than 80% of the N-terminus, from residues 28 through 283 ($Kv1.4_{\Delta 28\text{-}283}$) (Lee et al., 1994), did not significantly alter the rate of current inactivation (Fig. 1*A* and *B*). The major time constant describing the time course of current inactivation for Kv1.4 was 43 ± 6 msec ($n = 6$), while the major time constant for $Kv1.4_{\Delta 28\text{-}283}$ was 40 ± 6 msec ($n = 7$). Deletion of residues 2 through 283 ($Kv1.4_{\Delta 2\text{-}283}$), however, abolished fast current inactivation as can be seen in Fig. 1*C*. Rapid inactivation in Kv1.4, therefore, can be attributed entirely to a structural element located within the first 28 residues.

Inactivation Rate in Heteromultimeric Channels

We next examined current inactivation as a function of the number of Kv1.4 inactivation gates per channel. In contrast to Kv1.4 (Fig. 2*A*), Kv1.5 homomultimeric channels exhibited very little inactivation over 2 sec (Fig. 2*B*). Therefore, we varied the number of inactivating subunits per channel by forming heteromultimeric channels between Kv1.4 and Kv1.5. We examined current kinetics in two heteromultimeric channel types: (i) channels formed from a fusion gene linking the 3′ end of Kv1.4 to the 5′ end of Kv1.5 in a single open reading frame [tandem construct, (Lee et al., 1994), Fig. 2*C*], and (ii) channels formed in coinjection experiments where Kv1.5 was expressed in vast excess (32:1 Kv1.5:Kv1.4 coinjections, Fig. 2*D*). All heteromultimeric current types exhibited a transient current, consistent with channels containing inactivating Kv1.4 subunits.

Kv1.4 and Kv1.5 differed sufficiently in their midpoints of steady-state availability such that this difference could be employed to determine heteromultimeric

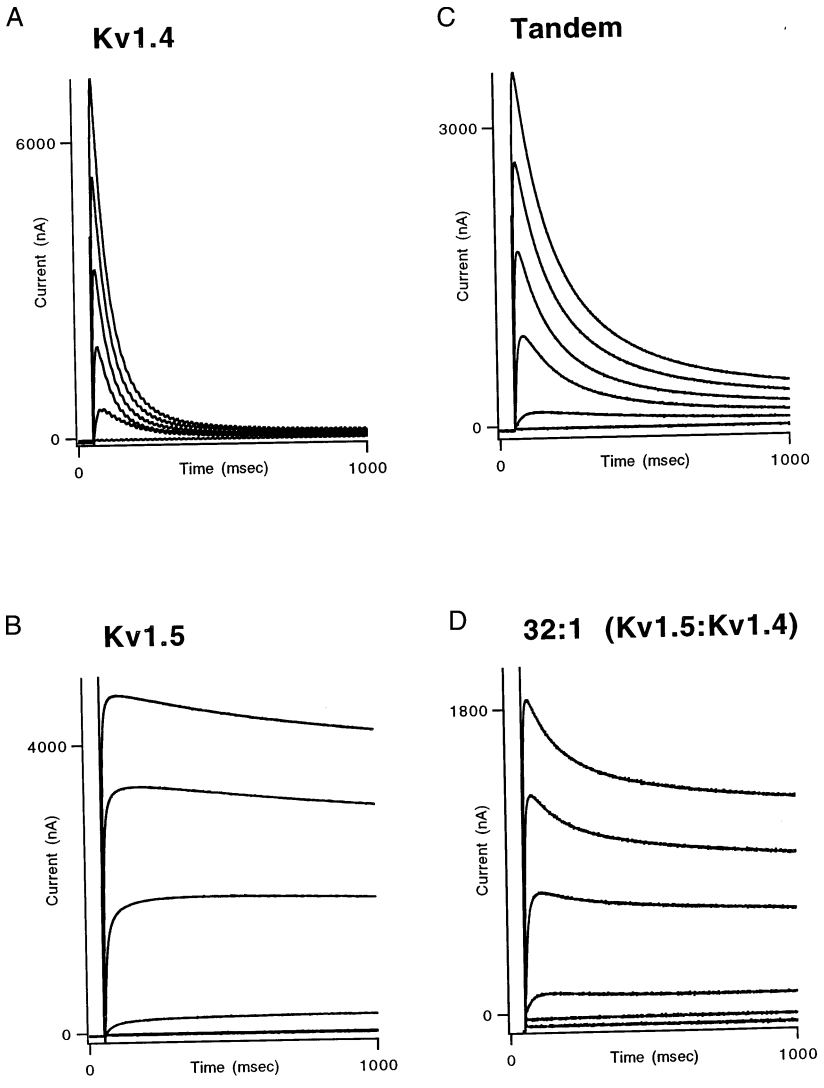

Fig. 2. Comparative time course of current inactivation for Kv1.4, Kv1.5, and heteromultimeric K^+ channels. (*A*) Representative currents recorded from a*Xenopus* oocyte injected with cRNA encoding Kv1.4. (*B*) Current recorded from an oocyte injected with Kv1.5 cRNA. (*C*) Current recorded from the tandem construct of Kv1.4 and Kv1.5. (*D*) Current recorded from an oocyte coinjected with a 32:1 (Kv1.5:Kv1.4) ratio of cRNA. All currents were recorded during 1-sec depolarizing steps from −60 to +40 mV in 20 mV increments from a holding potential of −80 mV. The interpulse interval was 3 sec for Kv1.5 currents and 10 sec for all other currents. Currents are shown unsubtracted for leak or capacity transients.

channel subunit composition (Fig. 3*A*). The midpoint of steady-state availability measured from tandem cDNA heteromultimers was midway between that measured for Kv1.4 and Kv1.5 (Table 1), consistent with the formation of heteromultimers composed of two Kv1.4 subunits and two Kv1.5 subunits.

Current recorded in 32:1 (Kv1.4:Kv1.4) coinjection experiments was characterized by a small transient component and a large noninactivating component. The steady-state availability for the transient component was determined by subtracting the noninactivating current measured at the end of the 2-sec voltage step from the total current. The midpoint of steady-state availability for the transient current was shifted 7 mV positive from that measured for the tandem construct (Fig. 3*A*, Table 1). The positive shift in the midpoint of steady-state availability showed that these currents are generated from heterotetramers which contain one fewer Kv1.4 subunit.

To identify the noninactivating current in coinjection experiments, we measured the steady-state availability of the current remaining at the end of a 2-sec voltage step. In Fig. 3*B*, the steady-state availability curve measured for Kv1.5 was superimposed upon the noninactivating current in 8:1 (Kv1.5:Kv1.4) coinjection experiments, where fifty percent of the current remained at the end of a 2-sec voltage step to +40 mV, and in 32:1 (Kv1.5:Kv1.4) coinjection experiments, where eighty percent of the current remained at the end of the identical voltage step. The steady-state availability curves measured for the noninactivating current in both types of coinjection experiments were identical to that measured for Kv1.5 homomultimeric current, indicating that the noninactivating component in the coinjection experiments could be attributed exclusively to Kv1.5 homomultimeric channels.

We measured the steady-state availability of current from oocytes coinjected with eight times more Kv1.4

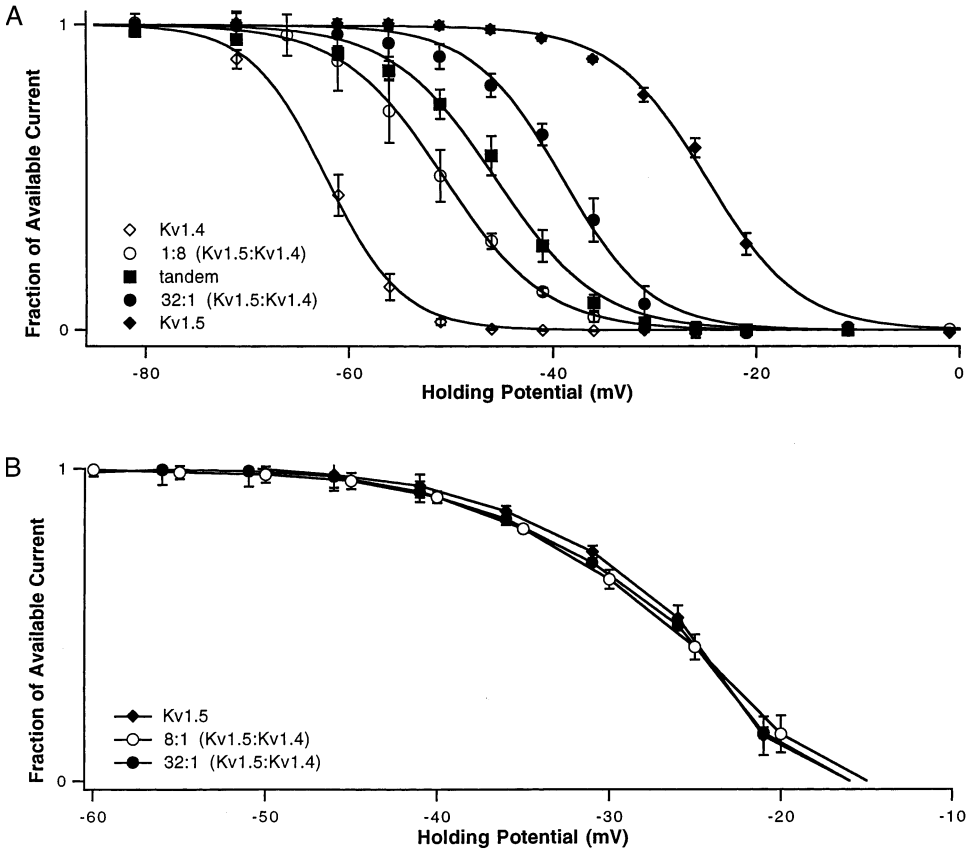

Fig. 3. Channel type can be identified by measuring steady-state availability. (*A*) Steady-state availability of currents from oocytes injected with Kv1.5 cRNA (average of 3 oocytes, filled diamonds), currents from oocytes injected with Kv1.4 cRNA (average of 5 oocytes, open diamonds), currents from oocytes injected with cRNA made from a tandem construct of Kv1.4 and Kv1.5 (average of 7 oocytes, filled squares), currents from 1:8 (Kv1.5:Kv1.4) coinjection experiments (average of 2 oocytes, open circles), and transient currents from 32:1 (Kv1.5:Kv1.4) coinjection experiments (average of 4 oocytes, filled circles). Steady-state availability curves were determined by fitting averaged data with a single Boltzmann isoform of the form $G_k(n) = G_{kmax}/(1 + \exp[V\text{-}V_{1/2}/k])$, where $V_{1/2}$ is the voltage at the midpoint of steady-state availability. The midpoint of the single curve was not significantly different from the average of the midpoints derived from the fitted curves for each cell. Values for steady-state availability of the transient currents recorded from the 32:1 (Kv1.5:Kv1.4) coinjection experiments were obtained by subtracting the noninactivating current measured at the end of 2-sec depolarizing voltage step from the total current. This same procedure, when applied to Kv1.4 homomultimeric or tandem currents, did not change their steady-state availability curves (*data not shown*). (*B*) Steady-state availability of current measured at the end of 2-sec voltage steps for oocytes injected with Kv1.5 cRNA (average of 3 oocytes, and filled diamonds), oocytes coinjected with an 8:1 (Kv1.5:Kv1.4) cRNA ratio (average of 3 oocytes, open circles), and oocytes coinjected with a 32:1 (Kv1.5:Kv1.4) cRNA ratio (average of 2 oocytes, filled circles). Curves shown represent straight lines drawn through the data points. For all curves, error bars indicate SEM. All steady-state availability measurements were made from currents evoked in 2-sec voltage pulses to +40 mV after holding at the indicated potential for 1 min.

than Kv1.5 cRNA (1:8 Kv1.5:Kv1.4 coinjection), to determine whether all subunit stoichiometries are generated in coinjection experiments. The midpoint of steady-state availability for currents from the 1:8 (Kv1.5:Kv1.4) coinjection experiments was intermediate between that measured for tandem currents and Kv1.4 homomultimeric currents (Fig. 3*A*, Table 1) consistent with a population of channels which contained three Kv1.4 subunits and one Kv1.5 subunit.

Previously, we have shown that comparison of steady-state availability curves for heteromultimeric currents recorded in coinjection experiments with curves

Table 1. Midpoints of steady-state availability as a function of channel type and subunit composition

Channel composition	Midpoint of steady-state availability (mV)	*n*
Kv1.4	−62 ± 1.5	5
1:8 (Kv1.5:Kv1.4)	−51 ± 1	4
Tandem	−45.6 ± 1.3	7
32:1 (Kv1.5:Kv1.4)	−39.0 ± 1.2	4
Kv1.5	−24.9 ± 0.6	3

The midpoint of steady-state availability was determined from Boltzmann fits to the data as described in the text.

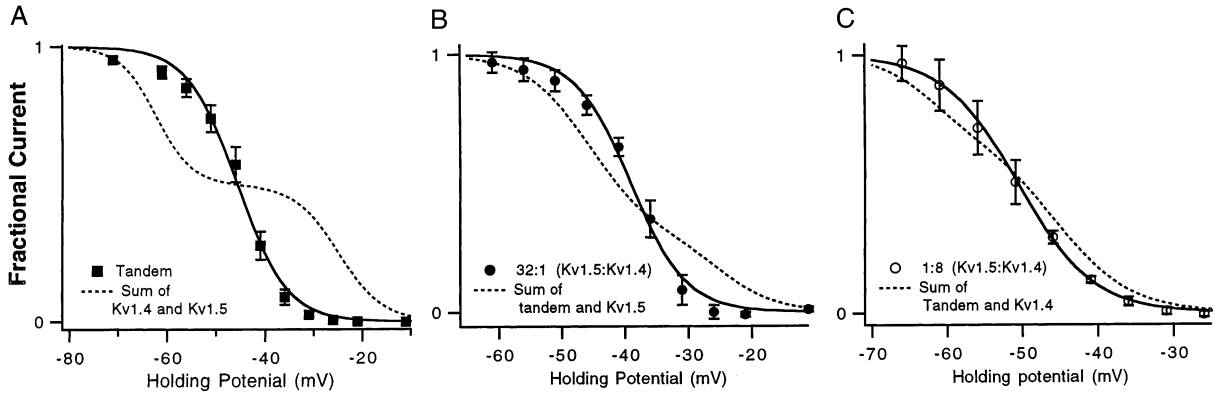

Fig. 4. Currents produced from coinjections and the tandem construct are from novel channel types. (*A*) Steady-state availability curve for the tandem (continuous line, filled squares) as compared to a waveform obtained by the digital addition of normalized steady-state availability curves from currents measured in oocytes injected with either Kv1.4 and Kv1.5 (broken line). (*B*) Steady-state availability curve measured for transient currents from the 32:1 (Kv1.5:Kv1.4) coexpression experiments (continuous line, filled circles) as compared to the digital sum of normalized steady-state availability curves measured for tandem and Kv1.5 currents (broken line). (*C*) Steady-state availability curve measured for current from the 1:8 Kv1.5:Kv1.4 coinjection experiments (continuous line, open circles) as compared to a digital sum of the steady-state availability curves measured for tandem and Kv1.4 currents (broken line). Steady-state availability curves, including those which have been digitally added, are the same as those shown in Fig. 3*A*. For all curves, error bars indicate SEM.

produced by the digital addition of availability curves obtained from homomultimeric Kv1.4 and Kv1.5 homomultimeric currents revealed the presence of novel heteromultimeric channel types (Lee et al., 1994). This approach, when applied to currents recorded from the tandem construct (Fig. 4*A*), demonstrated that the tandem current is produced from a single channel population and is not the result of the independent expression of Kv1.4 and Kv1.5. Similarly, steady-state availability curves measured in the 1:8 (Kv1.5:Kv1.4) coinjection experiments cannot be explained by the sum of tandemlike channels and Kv1.4 homomultimers (Fig. 4*B*). The transient current component measured in the 32:1 (Kv1.5:Kv1.4) coinjection experiments is, likewise, not equal to the that found in the sum of Kv1.5 homomultimers and tandemlike heteromultimers, but is the result of a different class of heteromultimeric channels (Fig. 4*C*).

Rate of Inactivation as a Function of Kv1.4 Subunits

We compared the rate of current inactivation in (i) heteromultimeric channels generated in the 32:1 (Kv1.5:Kv1.4) coinjection experiments, (ii) heteromultimeric channels from the tandem, and (iii) Kv1.4 homomultimeric channels. Channels in these experiments contain one, two, and four inactivation gates per channel, respectively. The time course of inactivation for all transient currents was well fit with a double exponential (Table 2). In Fig. 5*A*, the major time constants of current inactivation for the three current types are plotted as a function of the midpoint of steady-state availability, which reflects the expected number of inactivating subunits per channel. The time constant of inactivation for tandem heteromultimers which contain two inactivation gates per channel was double that determined for Kv1.4 homomultimers which contain four inactivation gates per channel. However, the time constant of inactivation for the transient current component recorded from the 32:1 (Kv1.5:Kv1.4) coinjection experiments was the same as that measured for tandem heteromultimers even though tandem channels contain twice the number of inactivating subunits per channel. The similarity in the inactivation time course between heteromultimers generated from the tandem and heteromultimers formed in the 32:1 (Kv1.5:Kv1.4) coinjection experiments is apparent in Fig. 5*B*. The time course of the transient current isolated from a 32:1 (Kv1.5:Kv1.4) coinjection experiment (Fig. 5*B*) was superimposible with that obtained from Kv1.4 homomultimers and heteromultimers formed from the tandem. Thus, a fourfold reduction in the number of Kv1.4 subunits resulted in only a two-fold reduction in the rate of current inactivation.

The Effect of Kv1.5 Coinjected with Noninactivating Kv1.4 on the Inactivation Rate

Differences in inactivation rates between channels with varying Kv1.4 - 1.5 stoichiometries could be due to gene-specific differences in the binding of the inactivation particle to the channel pore. We therefore compared currents in coexpression studies using Kv1.4 and its corresponding noninactivating deletion mutant with Kv1.4 - Kv1.5 heteromultimers.

Noninactivating $Kv1.4_{\Delta 2\text{-}283}$ subunits can not het-

Table 2. Kinetics of current inactivation as a function of channel subunit composition

Current type	Time constant for current inactivation (in msec)		Amplitude ratio	Cells	Inactivating subunits per channel
	$\tau 1$	$\tau 2$	$A_1/(A_1 + A_2)$		
Kv1.4	43 ± 6	117 ± 22	0.70 ± 0.09	6	4
Kv1.5	1156 ± 54[1]	690 ± 17	0.80 ± 0.04[1]	3	0
$Kv1.4_{\Delta 28–283}$	40 ± 6	159 ± 30	0.90 ± 0.05	7	4
Tandem	81 ± 4	271 ± 23	0.60 ± 0.07	4	2
32:1 (Kv1.5:Kv1.4)	72 ± 8	250 ± 115	0.56 ± 0.20	4	1
30:1 ($Kv1.4_{\Delta 28–283}$:$Kv1.4_{\Delta 28–283}$)	73 ± 9	610 ± 138	0.57 ± 0.06	5	1

[1] Data from (Philipson et al., 1991).

Inactivating heteromultimeric currents were isolated using the prepulse inactivation protocol as described in Materials and Methods. The time constants of inactivation (τ_1 and $+au_2$) and their respective amplitudes (A_1 and A_2) were determined from exponential fits to the current records. Current decays were analyzed as a sum of exponentials by a Fourier method (Provencher, 1976) that determined the number, amplitudes, and time constants of the components. Summary data are expressed as means ± SEM with the number of experiments in parentheses.

eromultimerize with wild-type Kv1.4 subunits, since $Kv1.4_{\Delta 2\text{-}283}$ subunits are missing the recognition sequence permissive for heteromultimerization within the Kv1.X subfamily (Lee et al., 1994). However, subunits which are missing the recognition sequence will heteromultimerize with other subunits which are also missing the recognition sequence (Lee et al., 1994). Therefore, we coinjected $Kv1.4_{\Delta 2\text{-}283}$ and $Kv1.4_{\Delta 28\text{-}283}$ cRNA to produce heteromultimers with inactivating and noninactivating Kv1.4 subunits. Heteromultimeric channels in oocytes with noninactivating $Kv1.4_{\Delta 2\text{-}283}$ subunits in large excess will predominantly contain a single inactivating $Kv1.4_{\Delta 28\text{-}283}$ subunit per channel assuming random assortment. We expressed $Kv1.4_{\Delta 2\text{-}283}$ subunits in excess by coinjecting 30-fold more cRNA relative to $Kv1.4_{\Delta 2\text{-}283}$ cRNA. The resulting transient current was compared with that obtained from 32:1 (Kv1.5:Kv1.4) coinjection experiments, and with the $Kv1.4_{\Delta 28\text{-}283}$ homomultimeric current (Fig. 6*A*).

Transient current isolated from the 30:1 ($Kv1.4_{\Delta 2\text{-}283}$:$Kv1.4_{\Delta 28\text{-}283}$) coinjection experiments could be fit well with two exponentials (Table 2). The major component of inactivation was similar to that measured in the 32:1 (Kv1.5:Kv1.4) coinjection experiments (Fig. 6*A*) and from the tandem construct Fig. 6*B*. These currents where also characterized by a large noninactivating component consistent with the large overexpression of noninactivating Kv1.4 subunits (Fig. 6*B* insert). The midpoint of inactivation for the two mutant channels was identical, preventing identification of the noninactivating component of the current in these experiments as $Kv1.4_{\Delta 28\text{-}283}$ homomultimeric current. The similarity between the major inactivation rate constants for transient current recorded in 32:1 (Kv1.5:Kv1.4) coinjection experiments and transient current recorded in the 30:1 ($Kv1.4_{\Delta 2\text{-}283}$:$Kv1.4_{\Delta 28\text{-}283}$) coinjection experiments indicates a consistent nonlinear relationship between the rate of current inactivation and the number of inactivating subunits per channel in these two combinations. Thus it did not matter if the noninactivating component was Kv1.5 or the noninactivating mutation of Kv1.4.

Discussion

We have investigated fast inactivation in homo- and heteromultimeric K^+ channels containing subunits from the mammalian *Shaker* gene, Kv1.4. By deleting residues from the N-terminus of Kv1.4, we found that the only structural element within the N-terminus that was required for fast inactivation was located within the first 27 residues. This result is consistent with deletion experiments reported elsewhere (Tseng & Tseng-Crank, 1992; Tseng-Crank et al., 1993).

We next examined inactivation by studying channels which were formed by combining inactivating Kv1.4 subunits with subunits of the noninactivating Kv1.5. Oocytes in which Kv1.5 and Kv1.4 genes were coexpressed produced currents with both a transient and a noninactivating component. The Kv1.5:Kv1.4 channel subunit stoichiometry which produced the transient current and the noninactivating current was determined by measuring the midpoint of steady-state availability. Transient currents recorded from a tandem (Kv1.4–Kv1.5) construct, 1:8, and 32:1 (Kv1.5:Kv1.4 cRNA) coinjections were produced from heteromultimeric channel types composed of 2:2, 3:1, and 1:3 Kv1.4:Kv1.5 subunits, respectively. Steady-state availability analysis showed that the noninactivating component of the current in coexpression experiments was due to Kv1.5 ho-

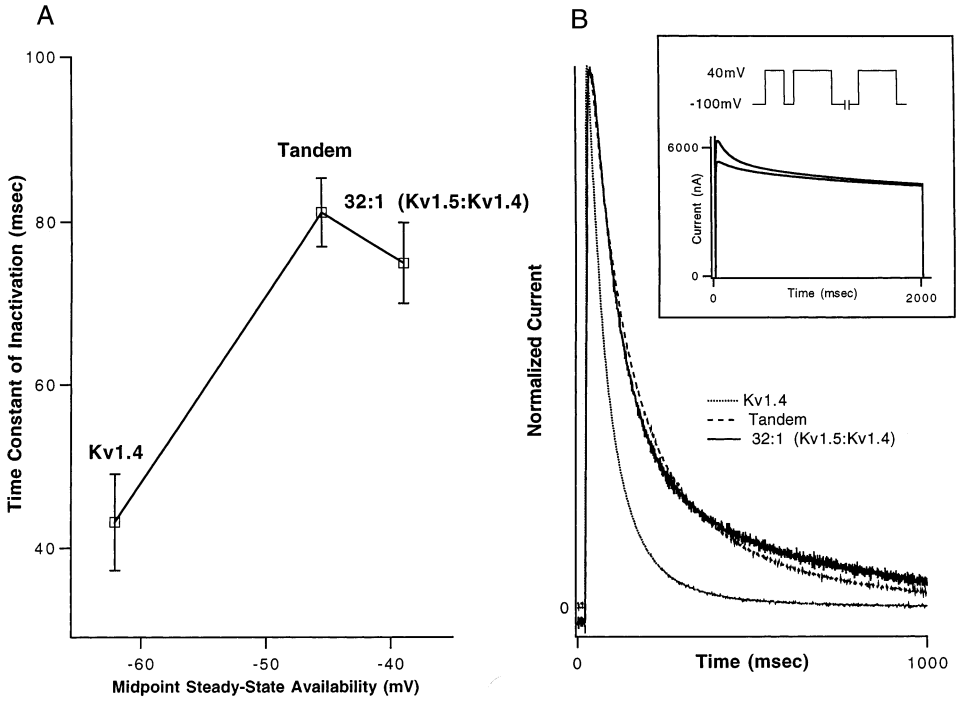

Fig. 5. Comparison of the rate of current inactivation from wild-type and heteromultimeric channels containing four, two, and one inactivating subunit. (*A*) Major time constant of inactivation taken from Table 2 for Kv1.4 homomultimeric current, current from oocytes injected with the tandem construct, and transient current form oocytes injected with 32:1 (Kv1.5:Kv1.4) cRNA plotted as a function of the midpoint for steady-state availability for each of the channel species. Error bars indicate SEM. (*B*) Comparison of time course of inactivation for current recorded from an oocyte injected with Kv1.4 (dotted line), current from an oocyte injected with the tandem construct (dashed line), and transient current recorded from 32:1 (Kv1.5:Kv1.4) coinjection experiments (solid line). Currents have been normalized to facilitate comparison. (*B insert*) Prepulse protocol used to isolate transient current from steady-state current and superimposed currents which have been evoked from the prepulse protocol in a 32:1 (Kv1.5:Kv1.4) coinjection experiment.

momultimeric channels. Therefore, a single Kv1.4 subunit conferred fast inactivation.

The major time constant for fast inactivation in channels containing four, two, and one inactivating Kv1.4 subunit was determined. Channels with four Kv1.4 subunits inactivated twice as fast as channels with two Kv1.4 subunits. Channels with two inactivating Kv1.4 subunits did not inactivate any faster than channels which contained only a single Kv1.4 subunits. Similar results were obtained with channels composed of inactivating and noninactivating deletion mutants of Kv1.4.

The mechanism of N-type inactivation in the *Drosophila* K^+ channel ShB has been examined previously (Hoshi et al., 1990; Murrell-Lagnado & Aldrich, 1993*a*, *b*; Zagotta et al., 1990). The N-terminal inactivation mechanism of ShB has been explained by the ''ball-and-chain'' hypothesis, in which inactivation occurs when an inactivation particle diffuses into and occludes the mouth of the open channel. Mutations that altered the putative peptide chain, thereby decreasing or increasing the local concentration of inactivation particles, resulted in decreased and increased rates of current inactivation, respectively (Hoshi et al., 1990). When the inactivation peptide was applied to the cytoplasmic side of ShB channels that were missing the N-terminal inactivation domain, the inactivation rate was proportional to the peptide concentration (Zagotta et al., 1990). Finally, in experiments similar to those we report here, decreasing the number of inactivating ShB subunits per channel decreased the rate of current inactivation in a linear manner (MacKinnon et al., 1993).

The N-terminal inactivation particle of the mammalian *Shaker* channel must function in a similar fashion, but some interesting differences may exist. Deletions within the ''chain'' region of the primary structure slowed, rather than increased, the inactivation rate in Kv1.4 (Tseng-Crank et al., 1993). Here we have demonstrated that complete deletion of the region corresponding to the ''chain'' was without effect on inactivation. Further, the rate of macroscopic current inactivation was not a linear function of the number of inactivating Kv1.4 subunits per channel.

In our analysis, we utilized a tandem cDNA construct to produce channels with only two inactivating Kv1.4 subunits per channel and found that the observed kinetics were consistent with such a channel structure. Linking K^+ channel subunits has been useful for exam-

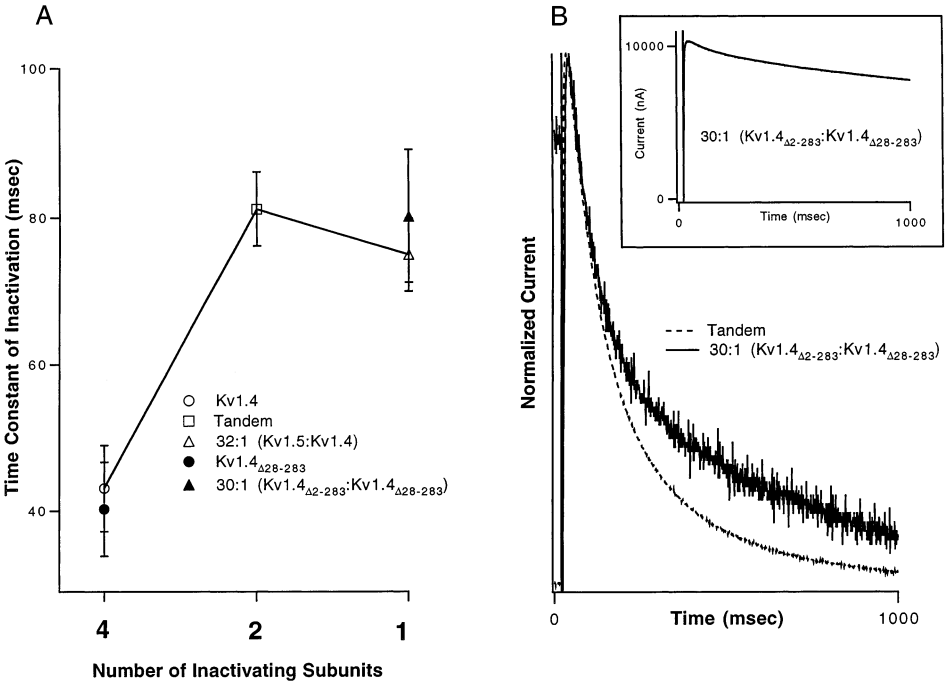

Fig. 6. Comparison of the rate of current inactivation in heteromultimers of N-terminal deletion mutant Kv1.4 channels. (*A*) Major time constant of inactivation taken from Table 2, for Kv1.4 homomultimeric current (open circles), $Kv1.4_{\Delta 28\text{-}283}$ homomultimeric current (filled circles), current from oocytes injected with the tandem construct (open squares), transient current from oocytes injected with 32:1 (Kv1.5:Kv1.4) cRNA (open triangles), and transient current form oocytes injected with 30:1 ($Kv1.4_{\Delta 2\text{-}283}$.$Kv1.4_{\Delta 28\text{-}283}$) cRNA (filled triangles) as a function of the predicted number of inactivating subunits per channel. Line drawn through same data points as in Fig. 5*A*. Error bars indicate SEM. (*B*) Current recorded from an oocyte injected with tandem cRNA (dashed line) and transient current isolated from an oocyte coinjected with 30:1 ($Kv1.4_{\Delta 2\text{-}283}$:$Kv1.4_{\Delta 28\text{-}283}$) cRNA (continuous line). Currents have been normalized to facilitate comparison. Steady-state current was eliminated using the prepulse subtraction protocol described in Materials and Methods and schematically portrayed in the insert to Fig. 5*B*. (*B insert*) Total current recorded in an oocyte coinjected with 30:1 ($Kv1.4_{\Delta 2\text{-}283}$:$Kv1.4_{\Delta 28\text{-}283}$) cRNA.

ining voltage-dependent kinetic properties (Liman, Tytgat & Hess, 1992; Tytgat et al., 1993) and N-type inactivation (Isacoff, Jan & Jan, 1990; Ruppersberg et al., 1991) in mixed subunit channels. While it has been reported that a tandem linkage does not necessarily guarantee the expected stoichiometry (McCormack et al., 1992), our analysis of steady-state availability for the tandem construct was consistent with a population of heteromultimeric channels with a 2:2 (Kv1.5:Kv1.4) stoichiometry. The significant advantage of the Kv1.4-1.5 tandem for this analysis is that the free amino terminal of the Kv1.4 subunits is freely available to associate with the inner face of the pore. The opposite tandem, Kv1.5-1.4, was not used in these experiments because it is likely that the amino terminal of Kv1.4 would be constrained by the C-terminal end of Kv1.5.

We have assumed in our investigations that subunits assort randomly. A similar assumption was made in the studies of MacKinnon and colleagues (MacKinnon et al., 1993) in their investigation of ShB K^+ channel stoichiometry. In our studies, as in the studies of ShB K^+ channels (MacKinnon, et al., 1993), both wild-type and mutant channels expressed with equal efficiently, consistent with the assumption that the relative amounts injected cRNAs induced a similar ratio in channel expression.

Separation of the midpoints of steady-state availability for currents expressed in the 1:8 and 32:1 (Kv1.5:Kv1.4) coinjection experiments suggests that heteromultimeric channels with predicted Kv1.5:Kv1.4 stoichiometries are formed, consistent with random assortment. Although we could not use steady-state availability as an assay of subunit stoichiometry for channels formed in the $Kv1.4_{\Delta 2\text{-}283}$ and $Kv1.4_{\Delta 28\text{-}283}$ coinjection experiments, it is also likely that these subunits assorted randomly. Random assortment should be enhanced in this combination since both deletion mutants are missing the conserved N-terminal domain important in the regulation of channel assembly (Lee et al., 1994; Shen et al., 1993). Elimination of this N-terminal region allows for assembly of subunits even from different subfamilies into heteromultimeric channels (Lee et al., 1994).

These results suggest that the model for N-type inactivation proposed for ShB need only be slightly modified to explain the inactivation kinetics exhibited by the mammalian channel Kv1.4. For Kv1.4, a single inactivation particle can bind to a site near the mouth of the

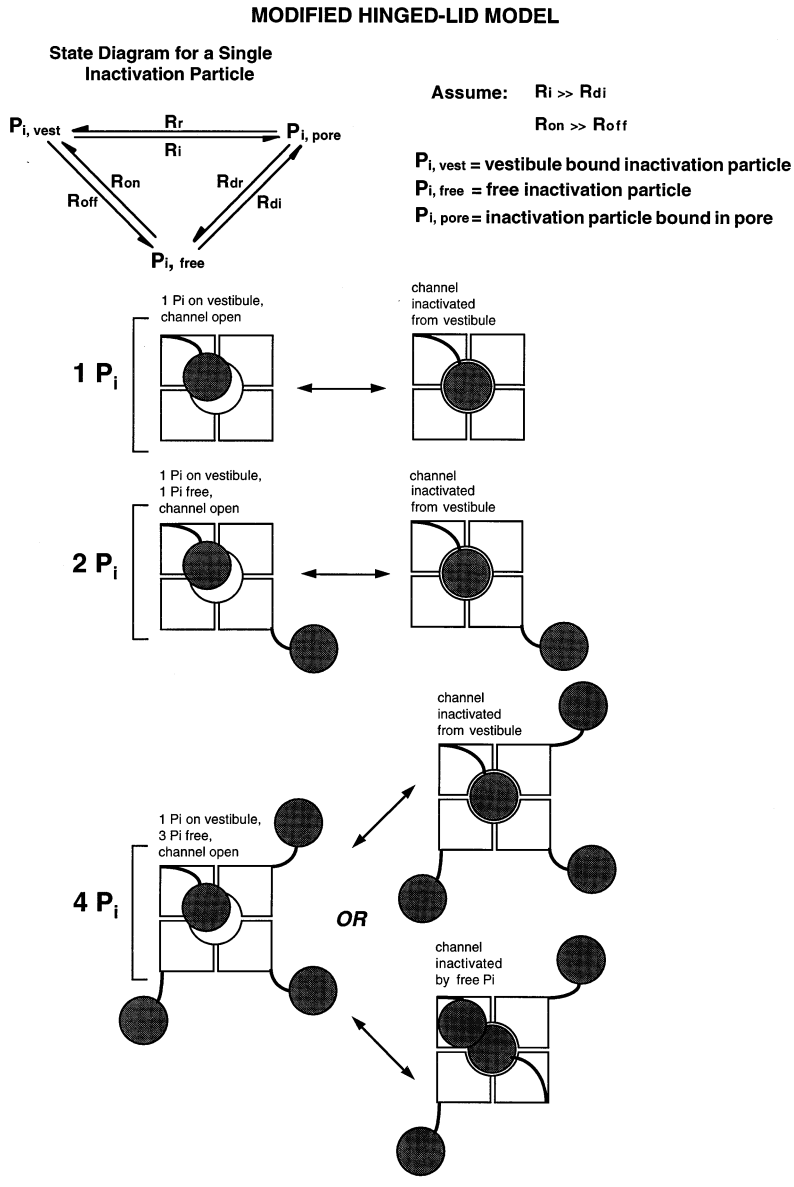

Fig. 7. Modified hinged lid model for mammalian *Shaker* K^+ channel inactivation. In this model, a single inactivation particle (P_i) can bind to a site at the mouth of the channel where there is room for only one particle, and only one inactivation particle can occupy the vestibule at a time. As seen in the state diagram, the model assumes that $R_{on} >> R_{off}$ and that $R_i >> R_{di}$ where R_{on} is the rate constant describing the conversion of the freely diffusible inactivation particle ($P_{i,free}$) to the vestibule bound ($P_{i,vest}$) state and R_{off} is the release of the particle from the vestibule bound state to the freely diffusible state. R_i is the rate constant describing the conversion of the particle from the vestibule-to the pore-bound state ($P_{i,pore}$), and R_{di} is the rate constant describing the movement of the particle from the freely diffusible state to the bound inactivated state. According to this model the inactivation rate is largely determined by the contribution of the particles bound to the docking or binding site in the vestibule when the concentration of free, unbound particles is low (*see text*).

channel where there is room for only one such particle at a time. Inactivation might then be thought of as a combination of the ''ball and chain'' with the ''hinged lid'' model, a model previously proposed for the inactivation of the voltage activated Na^+ channel (West et al., 1992). Such a mechanism might explain how a channel with two inactivation particles inactivates as fast as a channel with one inactivation particle, since only one inactivation particle can occupy the vestibule at a time. A modification of the simple hinged-lid model to include a much slower rate of inactivation by particles which are not bound to the vestibule (*see* Fig. 7), may explain the observation that Kv1.4 homomultimers with four potential inactivation particles exhibited a faster rate of current inactivation than the Kv1.4-Kv1.5 tandem containing two particles per channel. In our model we assume that $R_{on} >> R_{off}$ and therefore the vestibule site is constantly occupied. Assuming that inactivation by particles bound to the vestibule is much more efficient than free particles ($R_{di} << R_i$), then as long as the free concentration of particles is low, the inactivation rate is largely determined by the contribution of the particles bound to the vestibule. However, when the local concentration of free particles increases beyond the threshold of two, then the rate of inactivation by free particles can increase the overall rate of inactivation.

In conclusion, these studies suggest that a purely kinetic modification of the ''ball and chain'' hypothesis is sufficient to explain the differences in inactivation between the *Shaker* ShB channel and hKv1.4. Further

studies may identify the precise amino acid residues responsible for this variation.

The authors wish to thank A. Kusnetzov for preparation of the tandem construct. Funding was provided by the Marilyn M. Simpson Charitable Trust (to LHP). NIH Grant P01 DK44840 (to LHP and DJN), ADA Research and Development Award (to LHP), and R01 GM36823 and P01 NS24575 (to DJN).

References

Armstrong, C.M., Bezanilla, F. 1977. Inactivation of the sodium channel II. Gating current experiments. *J. Gen. Physiol.* **70:**567–590

Hoshi, T., Zagotta, W.N., Aldrich, R.W. 1990. Biophysical and molecular mechanisms of *Shaker* potassium channel inactivation. *Science* **250:**533–538

Isacoff, E.Y., Jan, Y.N., Jan, L.Y. 1990. Evidence for the formation of heteromultimeric potassium channels in *Xenopus* oocytes. *Nature* **345:**530–534

Isacoff, E.Y., Jan, Y.N., Jan, L.Y. 1993. Molecular basis of K^+ channel inactivation gating. *EXS* **63:**338–357

Jan, L.Y., Jan, Y.N. 1994. Potassium channels and their evolving gates. *Nature* **371:**119–122

Kozak, M. 1989. The scanning model for translation: an update. *J. Cell Biol.* **108:**229–241

Krieg, P.A., Melton, D.A. 1987. An enhancer responsible for activating transcription at the midblastula transition in Xenopus development. *Proc. Natl. Acad. Sci. USA* **84:**2331–2335

Lee, T.E., Philipson, L.H., Kuznetsov, A., Nelson, D.J. 1994. Structural determinant for assembly of mammalian K^+ channels. *Biophys. J.* **66:**667–673

Liman, E.R., Tytgat, J., Hess, P. 1992. Subunit stoichiometry of a mammalian K^+ channel determined by construction of multimeric cDNAs. *Neuron* **9:**861–871

MacKinnon, R., Aldrich, R.W., Lee, A.W. 1993. Functional stoichiometry of Shaker potassium channel inactivation. *Science* **262:**757–759

Marcus-Sekura, C.J., Hitchcock, M.J. 1987. Preparation of oocytes for microinjection of RNA and DNA. *Methods Enzymol.* **152:**284–288

McCormack, K., Lin, L., Iverson, L.E., Tanouye, M.A., Sigworth, F.J. 1992. Tandem linkage of *Shaker* K^+ channel subunits does not ensure the stoichiometry of expressed channels. *Biophys. J.* **63:**1406–1411

Murrell-Lagnado, R.D., Aldrich, R.W. 1993*a*. Energetics of *Shaker* K channels block by inactivation peptides. *J. Gen. Physiol.* **102:**977–1003

Murrell-Lagnado, R.D., Aldrich, R.W. 1993*b*. Interactions of amino terminal domains of *Shaker* K channels with a pore blocking site studied with synthetic peptides. *J. Gen. Physiol.* **102:**949–975

Philipson, L., Hice, R.E., Schaefer, K., LaMendola, J., Bell, G.J., Nelson, D.J., Steiner, D.F. 1991. Sequence and functional expression in *Xenopus* oocytes of a human insulinoma and islet potassium channel. *Proc. Natl. Acad. Sci. USA* **88:**53–57

Philipson, L., Schaefer, K., LaMendola, J., Bell, G.I., Steiner, D.F. 1990. Sequence of a human fetal skeletal muscle potassium channel cDNA related to RCK4. *Nucleic Acids Research* **18:**7160

Provencher, S.W. 1976. A Fourier method for the analysis of exponential decay curves. *Biophys. J.* **16:**27–41

Ruppersberg, J.P., Stocker, M., Pongs, O., Heinemann, S.H., Frank, R., Koenen, M. 1991. Regulation of fast inactivation of cloned mammalina I_K(A) channels by cysteine oxidation. *Nature* **352:**711–714

Shen, N.V., Chen, X., Boyer, M.M., Pfaffinger, P.J. 1993. Deletion analysis of K^+ channel assembly. *Neuron* **11:**67–76

Tseng, G.N., Tseng-Crank, J. 1992. Differential effects of elevating $[K]_o$ on 3 transient outward potassium channels: dependence on channel inactivation mechanisms. *Circ. Res.* **71:**657–672

Tseng-Crank, J., Yao, J.-A., Berman, M.F., Tseng, G.-N. 1993. Functional role of the NH2-terminal cytoplasmic domain of a mammalian A-type K channel. *J. Gen. Physiol.* **102:**1057–1083

Tytgat, J., Hess, P. 1992. Evidence for cooperative interactions in potassium channel gating. *Nature* **359:**420–423

Tytgat, J., Nakazawa, K., Gross, A., Hess, P. 1993. Pursuing the voltage sensor of a volt-age-gated mammalian potassium channel. *J. Biol. Chem.* **268:**23777–23779

West, J.W., Patton, D.E., Scheuer, T., Wang, Y., Goldin, A.L., Catterall, W.A. 1992. A cluster of hydrophobic amino acid residues required for fast Na(+)-channel inactivation. *Proc. Natl. Acad. Sci. USA* **89:**10910–10914

Zagotta, W.N. Hoshi, T., Aldrich, R.W. 1990. Restoration of inactivation in mutants of *Shaker* potassium channels by a peptide derived from ShB. *Science* **250:**568–571